Silver Nanoparticles Capped by Long-Chain Unsaturated Carboxylates

Wei Wang,[†] Xiao Chen,[‡] and Shlomo Efrima*

Department of Chemistry, Ben-Gurion University of the Negev, Beer-Sheva 84105, Israel

Received: March 30, 1999; In Final Form: June 14, 1999

We study the preparation and capping of silver nanoparticles by several unsaturated long-chain carboxylates. UV−visible and FTIR spectroscopy and high-resolution electron microscopy are used to characterize the effect of the chain length, its configuration, and the degree of unsaturation on the size distribution of the nanoparticles. Langmuir layers and Langmuir−Blodgett films are used to study the adsorption of these carboxylates on the particles. We find that unsaturated carboxylates in the cis configuration are useful stabilizers for the control of particle size and its surface properties.

Introduction

Nanometer-sized particles of metals and semiconductors have been investigated intensively in recent years because of their size-dependent properties and the possibility of arranging them in micro (and nano) assemblies.[1] Intriguing prospects for the development of novel electronic devices, electrooptical applications, and also catalysis have been suggested.[2]

A variety of methods can be used for the formation of ultrasmall metal crystallites, such as molecular beam epitaxy,[3] chemical vapor deposition,[4] reduction by ionizing radiation,[5] thermal decomposition in organic solvents,[6] chemical or photo reduction in reverse micelles,[7] and chemical reduction with[8] or without[9] stabilizing polymers. From all this work, it can be assessed that colloidal stability, particle size, and properties depend strongly on the specific method of preparation and the experimental conditions applied. This, of course, is related to the inherent instability of the particles toward aggregation.

Silver nanocrystallites, mostly hydrosols, have been widely studied because of the ease of their preparation and stabilization and due to their application as catalysts[10] and their role in photographic processes[11] and as substrates for surface-enhanced Raman spectroscopy.[12]

We have developed a solvent exchange method which can be used to prepare a relatively high concentration of hydorosols and organosols composed of silver nanoparticles using oleate as a stabilizer.[13] We also noted the self-organization of silver particles with 2D hexagonal arrangements upon deposition and discussed the conformation of the oleate molecules adsorbed on the silver cores and the changes that enable the particles to transfer into the organic environment.[13]

To gain a better understanding of the function of the stabilizer molecules on the particles, we investigate in the present report the interactions between silver nanoparticles and several unsaturated and poly-unsaturated carboxylates.

Experimental Section

1. Materials. $AgNO_3$ (99+%), $NaBH_4$ (99%), $NaH_2PO_4 \cdot H_2O$ (98+%), cyclohexane (99.5%), oleic acid (99%), elaidic acid (98%), palmitoleic acid (98%), linoleic acid (99%), linolenic acid (99%), and *cis*-11-eicosenoic acid are purchased from Aldrich. Sodium oleate (99+%, GC), stearic acid (99+%), and sodium stearate (99+%, GC) are obtained from Sigma. NaBr (>99%) is a Fluka reagent. H_3PO_4 (85%) is a Merck product, and eosin is from BDH. NaOH (A.R.), HNO_3 (A.R.), and chloroform (A.R.) are provided by Frutarom. All the chemicals are used as received. Sodium salts of some unsaturated acids are prepared by stoichiometrically reacting the corresponding acids with sodium hydroxide in aqueous solutions. Silver salts are formed by mixing $AgNO_3$ and sodium carboxylate solutions with excess $AgNO_3$. Water is of ∼18 MΩ cm resistance, obtained from a Barnstead E-pure water purifier.

2. Preparation of Colloids. Native silver colloids without any additional stabilizer are prepared according to ref 14. One part ice cold 1×10^{-3} M $AgNO_3$ and another equal volume of 4×10^{-3} M $NaBH_4$ are mixed dropwise, with stirring, forming a clear yellow sol almost immediately. The sol is continuously stirred while allowing it to warm to room temperature.

Typically, unsaturated long-chain carboxylate-stabilized silver colloids are prepared as follows.[13] We add 25 mL of 5×10^{-3} M $AgNO_3$ into 25 mL of 2×10^{-2} M freshly prepared $NaBH_4$ containing 6.25×10^{-4} M unsaturated carboxylate stabilizer, with vigorously stirring at an ice-cold temperature. Brown-yellowish colloidal solutions stabilized by the carboxylates are obtained. Hydrophobic silver colloids are obtained by phase transfer induced by H_3PO_4 or NaH_2PO_4 in hydrosol−organic solvent biphasic mixtures. Some residues of the colloids concentrate at the liquid/liquid interface, forming an interfacial colloid or an interfacial powder deposit. The particles transfer ratios are estimated by comparing the integrated plasmon band in the UV−visible spectra of the aqueous phase just before the solvent exchange and that of the organosol after transfer.

3. Measurements. UV−visible spectra are taken with a 8452A HP diode array spectrophotometer in the range 190−820 nm, with a resolution of 2 nm. A variable path cuvette with quartz windows is used. Cast films from the Ag colloids are made by spreading a drop of the sol on a quartz plate and letting it dry.

Direct imaging of the particles is obtained by a JEOL 1200 EXII electron microscope under an acceleration voltage of 200 kV. A drop of the silver colloids is placed on a holey carbon film supported by a 300 mesh copper grid (TED PELLA-LTD,

* To whom correspondence should be addressed.
[†] Current address: Department of Chemistry, University of Pittsburgh, Pittsburgh, PA 15260.
[‡] Permanent address: Institute of Colloid and Interface Chemistry, Shandong University, Jinan, Shandong, 250100, P. R. China.

10.1021/jp991101q CCC: $18.00 © 1999 American Chemical Society
Published on Web 08/05/1999

TABLE 1: Stabilizer Molecules Investigated in This Study ($[Ag^+] = 2.5 \times 10^{-3}$ M; $[Ag^+]/[BH_4^-] = 4$; $[Ag^+]/[BH_4^-] = 0.25$)

name	formula	configuration	stability in water	transfer ratios from water into chloroform
oleate	$CH_3(CH_2)_7CH{=}CH(CH_2)_7COONa$	C18, cis	>3 months	40−50%
elaidate	$CH_3(CH_2)_7CH{=}CH(CH_2)_7COONa$	C18, trans	1−3 weeks	<10%
linoleate	$CH_3(CH_2)_4(CH{=}CHCH_2)_2(CH_2)_6COONa$	C18, two double bonds (cis, cis)	1−2 months	20−30%
linolenate	$CH_3(CH_2CH{=}CH)_3(CH_2)_7COONa$	C18, three double bonds (cis, cis, cis)	1−2 months	10−20%
palmitoleate	$CH_3(CH_2)_5CH{=}CH(CH_2)_7COONa$	C16, cis	>3 months	30−40%
eicosenoate	$CH_3(CH_2)_7CH{=}CH(CH_2)_9COONa$	C20, cis	>3 months	40−50%
stearate	$CH_3(CH_2)_{16}COONa$	C18, saturated	several days	∼0%

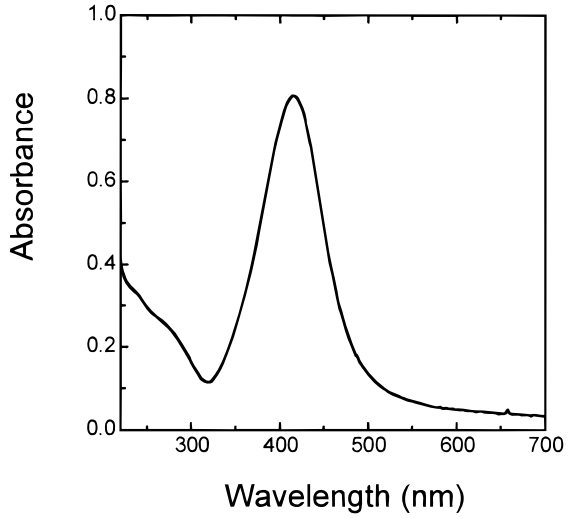

Figure 1. Typical UV−vis spectrum of an oleate-capped silver colloid suspension with $[Ag] = 5 \times 10^{-4}$ M.

Cat # 01883-F), and the solvent is allowed to evaporate. The size distribution of the silver particles is obtained by measuring the digitized micrographs. The mean diameter, D, and the standard deviation, σ, are derived from an average of ∼300 particles. The polydispersity is defined as the ratio σ/D.

Infrared spectra are recorded at 4 cm^{-1} resolution with a Nicolet Impact 410 FTIR spectrometer. The silver colloids are spread on KRS-5 windows and dried.

Surface pressure (π)/area (A) curves are measured in a Labcon Mini Langmuir trough at 21 ± 0.5 °C. The compression and expansion speeds for monolayers are 100 cm^2/min. Compression starts 5 min after spreading of the hydrophobic colloid particles in suspension, allowing evaporation of the solvent. Y-type LB films are deposited by vertical dipping using a speed of 4 mm/min. The concentration of the silver particles is evaluated based on the concentration of the silver in the chloroform and the average particulate diameters given by TEM. The concentration of the silver in chloroform was determined as follows.[15] A known volume of the organosol is evaporated, and the dried silver particles deposit is dissolved in nitric acid and then titrated by NaBr using eosin as an adsorption indicator.

Results and Discussion

1. Properties of the Colloids Capped by Different Stabilizers. Using oleate as a stabilizer, and keeping the molar ratios $[Ag^+]/[BH_4^-] = 0.25$ and $[Ag^+]/[\text{stabilizer}] = 4$, we produce colloids with various initial concentrations of silver ions. Figure 1 shows the characteristic UV−vis absorption of the hydrosol of oleate-capped silver nanoparticles. The extinction band for silver concentrations in the range 3.75×10^{-5} to 5.0×10^{-3} M appears at 413 ± 1 nm with a full width at half-maximum (fwhm) of 90 ± 2 nm, characteristic of rather monodispersed small silver particles,[16,17] while uncapped silver colloid exhibits absorption with a maximum at 390 nm. The shift of the absorption band provides clear evidence for the adsorption of oleate on the silver particles.[18,19] The bands at 413 ± 1 nm are rather symmetric with a constant width, demonstrating that particle sizes do not depend on the silver concentration. In contradiction to that, at $[Ag^+] \geq 1 \times 10^{-2}$ M, the absorption bands of the hydrosols become more asymmetric and blue shifted (to 408 nm at 1×10^{-2} M and to 400 nm at 2×10^{-2}

TABLE 2: IR Vibrational Frequencies of Unsaturated Carboxylates in Their Crystalline State and on Hydrosols and Organosols of Silver Nanoparticles[a]

		observed frequencies, cm^{-1}			
surfactant	status	ν_s, =C−H	ν_{as}, CH_2	ν_s, CH_2	ν_s, COO^-
eicosenoate	sodium salt	3004w	2921vs	2848s	1558vs
	silver salt	3008w	2919vs	2850s	1519vs
	hydrosol	3010w	2918vs	2850s	1558vs
	organosol	3003w	2924vs	2852s	1558w, 1709s
oleate	sodium salt	3002w	2921vs	2851s	1560vs
	silver salt	3004w	2923vs	2851s	1517vs
	hydrosol	3013w	2922vs	2852s	1559vs
	organosol	3003w	2922vs	2852s	1547m, 1709m
palmitoleate	sodium salt	3006w	2921vs, 2935sh	2850s	1560vs
	silver salt	3004w	2920vs	2850s	1516vs
	hydrosol	3013w	2921vs, 2935sh	2850s	1560vs
	organosol	3006w	2926vs	2855s	1558w, 1712s
linoleate	sodium salt	3010m	2921vs, 2935sh	2851s	1560vs
	silver salt	3008m	2925vs	2850s	1518vs
	hydrosol	3012m	2921vs, 2935sh	2851s	1560vs
	organosol	3010m	2927vs	2856s	1558w, 1711s
linolenate	sodium salt	3010s	2921vs, 2936sh	2849s	1560s
	silver salt	3010m	2925vs	2850s	1518vs
	hydrosol	3013m	2920vs, 2935sh	2849s	1560s
	organosol	3010m	2927vs	2855s	1558w, 1712s
elaidate	sodium salt	3140m	2917vs, 2933sh	2845s	1575vs
	silver salt		2919vs	2848s	1518vs
	hydrosol	3141m	2916vs, 2932sh	2843s	1567vs
	organosol		2918vs, 2943w	2848s	1558w, 1714s
stearate	sodium salt		2918vs	2849s	1558vs
	silver salt		2916vs	2848s	1518vs
	hydrosol		2918vs	2848s	1562sh, 1618s

[a] vs, very strong; s, strong; m, middle; w, weak; sh, shoulder; ν_{as}, asymmetric stretching; ν_s, symmetric stretching.

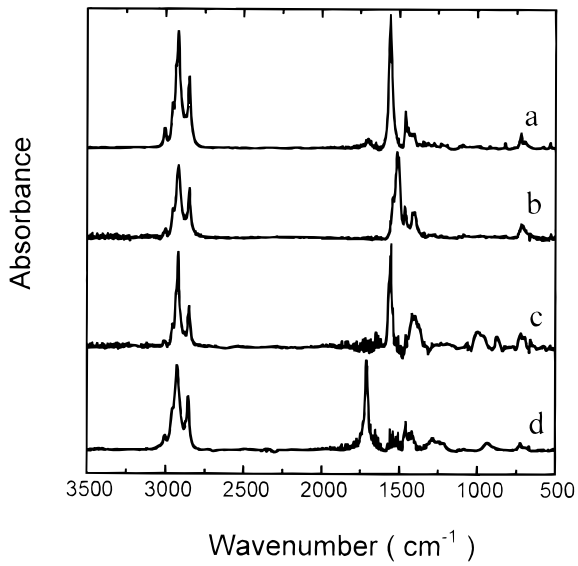

Figure 2. FTIR spectra for (a) sodium palmitoleate, (b) silver palmitoleate, (c) palmitoleate-capped silver hydrosol, and (d) palmitoleate-capped silver organosol. The samples are deposited on a KRS-5 window.

M) with a considerable increase of the fwhm (to 114 and 146 nm, respectively), indicating an increase of polydispersity and aggregation.

Accordingly, we choose $[Ag^+] = 5 \times 10^{-3}$ M as the silver ion concentration used to produce all the hydrosols we discuss in the following, giving a final concentration of $[Ag] = 2.5 \times 10^{-3}$ M due to a 2-fold dilution in the process. Usually, we use a constant molar ratio of $[Ag^+]/[\text{stabilizer}] = 4$ or 8 and $[Ag^+]/[BH_4^-] = 0.25$. Table 1 lists the long-chain carboxylates we used as stabilizers for the colloids, along with their molecular formula and additional information regarding the molecular configuration.

Stable silver suspensions are obtained using any of the stabilizers listed in Table 1 even at a high $[Ag^+]$ concentration of 1×10^{-2} M, while 1×10^{-3} M is too high for obtaining stable colloids in the absence of the stabilizer. All these colloids exhibit the characteristic extinction of small monodispersed silver particles at 412 ± 2 nm. The sols are stable from over several months down to a few weeks, depending on the specific stabilizer used. An exception is stearate which gave only short-term stability (a few days) with a concomitant degradation of the UV−visible spectrum. The various preparations exhibit a stability sequence as given in Table 1.

From the stability, we can infer the following points. (1) An unsaturated chain is essential for these long-chain carboxylates to effectively stabilize silver particles. A saturated chain (stearate) probably hardly adsorbs on the silver particles in an aqueous phase. The UV−visible spectrum of a colloid capped with stearate is blue-shifted toward the position of the uncapped colloid (390 nm), with respect to the position observed with the unsaturated molecules (412 nm). (2) The length of the chain (between C16 and C20) for unsaturated carboxylates does not have any significant effect on the stability. (3) Multiple double bonds do not perform as well as a single double bond in the chain. This might be attributed to the higher rigidity of the polyunsaturated molecules, which would make it more difficult to form a compact layer. (4) A trans configuration is not effective in stabilizing (adsorbing on) silver particles. In fact, the band for the =C−H stretch in the IR spectrum of the hydrosol when elaidate is used appears at practically the same position as for the pure compound. In contradiction, the band shifts when the cis isomers are used (Table 2). This might be an indication of weak adsorption of the trans isomer.

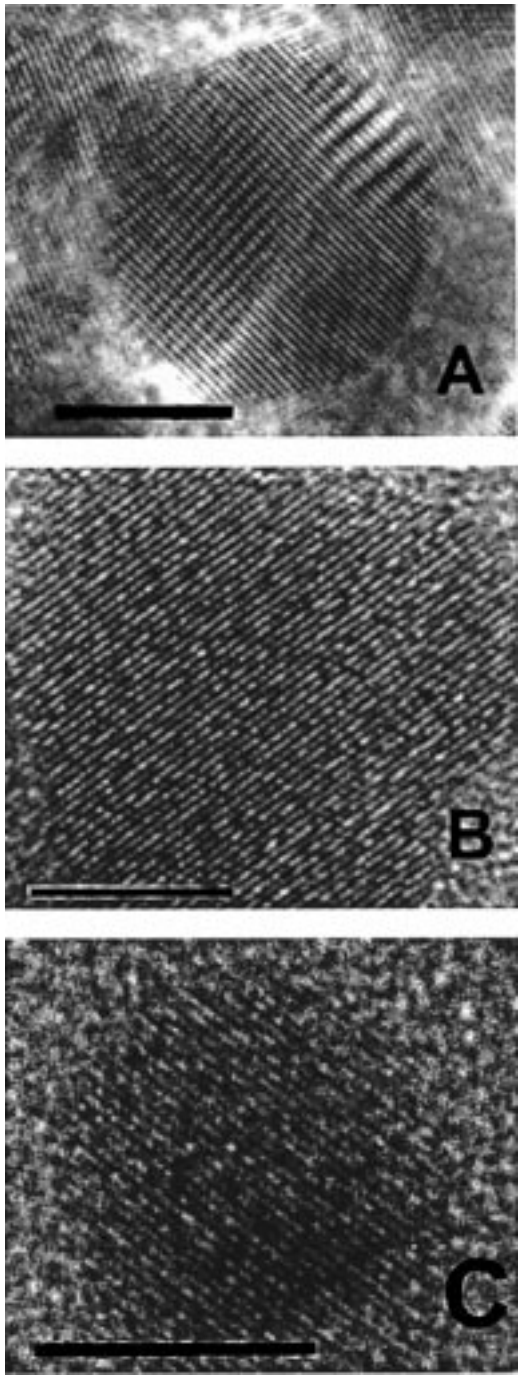

Figure 3. High-resolution transmission electron microscopy of organosol silver particles capped with (a) oleate, (b) palmitoleate, and (c) linoleate. The bar denotes 5 nm.

Using a method described earlier,[13] the capped silver particles can be transferred in part from the aqueous environment into various organic solvents.

A variety of organic solvents have been tried for such an interphase exchange process. They include cyclohexane, chloroform, hexane, isooctane, decane, dodecane, benzene, chlorobenzene, dichloromethane, carbon tetrachloride, chloropropane, chlorobutane, bromopropane, and dichloroethane. One can harvest the colloids as dry powders by evaporating the organic solvent, and they still retain their integrity. They can be redispersed in organic solvents producing stable colloids with extinction spectra very similar to the original ones.

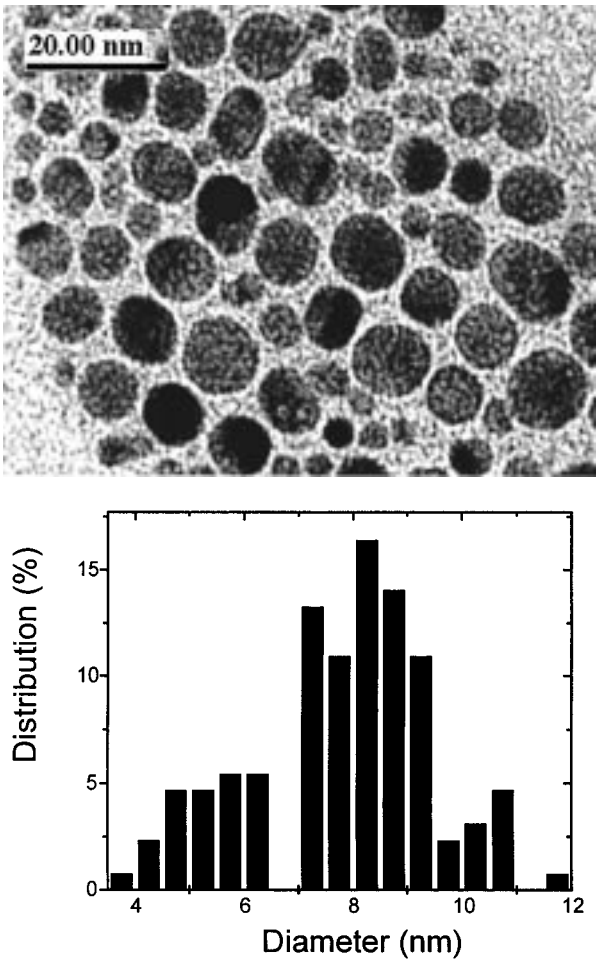

Figure 4. Transmission electron micrograph and histogram of *cis*-11-eicosenoate-capped silver particles from a colloidal dispersion in cyclohexane. [Ag]/[stabilizer] = 8.

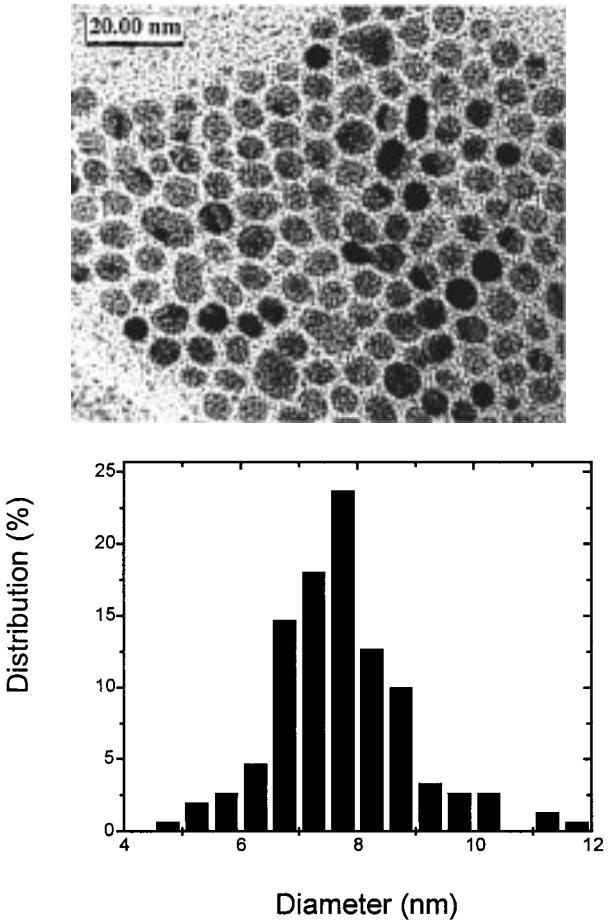

Figure 5. Transmission electron micrograph and histogram of *cis*-11-eicosenoate-capped silver particles from a colloidal dispersion in cyclohexane. [Ag]/[stabilizer] = 4.

The transfer ratios of silver particles from the aqueous phase to the organic one are sensitive to the stabilizer, as well as to the organic solvent. Table 1 shows the transfer ratios from the aqueous phase to chloroform for the various stabilizers. The trend parallels that observed for the hydrosol stability. Similar sequences are found for all the organic liquids listed above, though the precise value of the transfer ratio varies.

Absorption spectra of these organosols still retain the symmetric and narrow absorption band, but the absorption maxima red shift by 2−6 nm, depending on the specific organic solvent. We find an increase in the red-shift with an increase in the solvent refractive index, as expected from Mie theory. This confirms that the silver particles are still well-separated and monodisperse in the organosols after the solvent exchange.

2. Infrared Spectroscopy. To understand the role of the stabilizers in the formation of the colloids and their stabilization, FTIR spectra of the capped colloids are measured and compared with those of the sodium and silver carboxylates. Figure 2 shows typical spectra, here of sodium and silver palmitoleate, and its capped silver hydrosol and organosol particles. In all the spectra, one can identify the asymmetric and symmetric stretching bands of CH_2 and CH_3 around 2920/2850 cm^{-1}, or around 2953/2872 cm^{-1}, respectively.[20] These band positions are similar to those observed in the stearate spectrum. The CH_2 scissoring and in-phase rocking bands appear around 1464 and 722 cm^{-1}, respectively.[20] Thus, the stabilizer molecules are definitely associated with both the hydrosol and the organosol silver colloidal particles. A few of the important vibrational frequencies are summarized in Table 2. For the unsaturated carboxylates, the ═C−H and COO^- stretching bands appear, respectively, around 3005 and 1560 cm^{-1}. In the hydrosols, the frequency of the ═C−H stretch mode is consistently blue shifted by 2−11 cm^{-1}. There is almost no change, however, in the position of the COO^- stretching band compared to the sodium carboxylates, though this band is red shifted to ∼1518 cm^{-1} in the corresponding silver salts. An exception is the elaidate-capped hydrosol, which contains a trans double bond. Its COO^- band shifts by 8 cm^{-1} to higher energies, though its silver salt still shows a band at 1518 cm^{-1}, as in the silver salts of the other molecules studied here. The ═C−H stretch with elaidate hardly changes. These findings indicate that on the particles in the hydrosol there is a strong interaction between the cis C═C bond of the adsorbed unsaturated molecules and the silver surface. Consequently, the carboxylate group (COO^-) is far away from the surface, exposed to the external environment. The behavior of eladiate suggests that a cis configuration is necessary for effective adsorption. Apparently, the trans isomer has quite a different interaction with the silver particle, differing probably in the packing and the steric effect. In the case of the stearate anion, only the carboxylate functional group is available for anchoring to the silver surface. The IR spectrum shows that the carboxylate is indeed affected to a large extent.

In contrast, with the hydrophobic particles, the ═C−H stretch band remains at the same position as in the sodium salt, while the COO^- stretch shifts to around 1710 cm^{-1}, close to that of corresponding free acids, though residual bands around 1560 cm^{-1} are still observed. This is clear evidence that the double

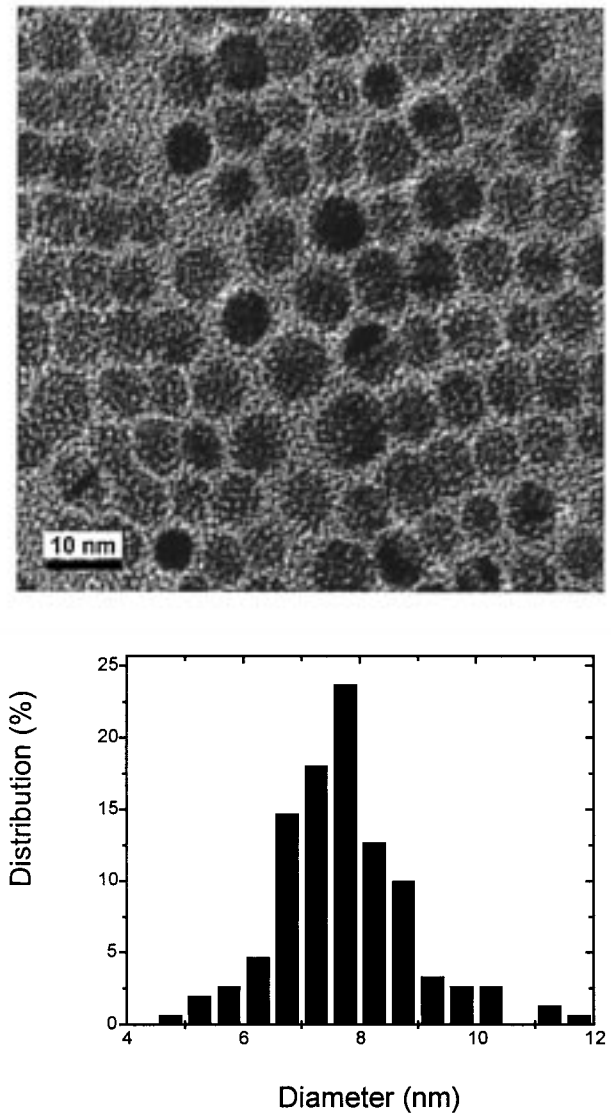

Figure 6. Transmission electron micrograph and histogram of oleate-capped silver particles from a colloidal dispersion in cyclohexane. [Ag]/[stabilizer] = 8.

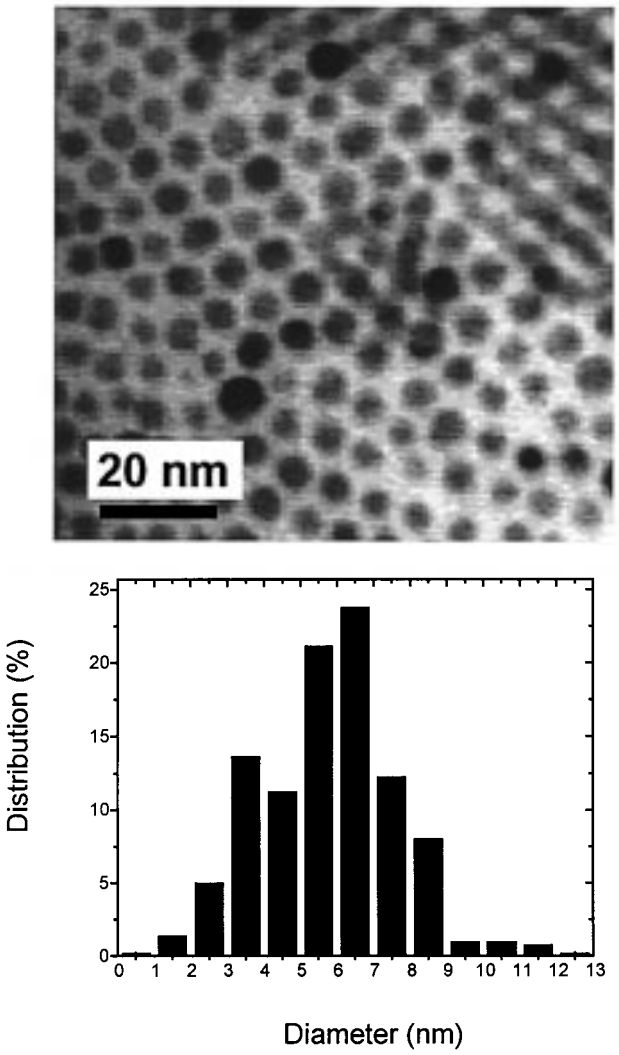

Figure 7. Transmission electron micrograph and histogram of oleate-capped silver particles from a colloidal dispersion in cyclohexane. [Ag]/[stabilizer] = 4.

bond which is adsorbed on silver particles in hydrosols is released after the solvent exchange, while the carboxylate group becomes attached to the surface. This also suggests that adsorption on particles in the organosols is mostly by carboxylic acid molecules rather than by dissociated carboxylates. Indeed, the phase transfer is carried out at a pH of 4−5 when the acid form is prevalent. Thus, the carboxylate group serves to anchor the stabilizers to the particle surface in the organosol, and subsequently the hydrophobic "tail" is directed toward the solvent. This holds for all the molecules we investigate here, except for the trans isomer. We find that this molecule (elaidate) produces the least stable colloid, and the lowest transfer ratio (except for the saturated stearate). Apparently, the trans structure makes it difficult for this molecule to adsorb on the particles and stabilize them.

An additional observation, in support of the structures suggested by the previous consideration, is the following. While the positions of the CH_2 and CH_3 stretches hardly change between the sodium salt and the hydrosol, in the organosol they blue-shift by 5 cm^{-1} (with minor exceptions). This can be attributed to a higher state of fluidity of the hydrocarbon chain in the organosol.[21] Pluasibly the better sovating properties of the organic liquid, would let it penetrate into the external hydrophobic region of the stabilizer layer and also allow its extension to its fullest length. In that fashion, the adsorbed layer is as least compact as possible, and the layer itself will be more fluid. In the hydrosols, in contradistinction, the penetration of water into the stabilizer layer on the particles is less likely. The sodium salt is a crystal, which again is compact and obviously not fluid.

3. Transmission Electron Microscopy Observation. Figures 3−10 show TEM pictures and size distributions of dried silver particles taken from the corresponding cyclohexane organosols using the various stabilizers. High-resolution electron micrographs (Figure 3) reveal spherical particles with the characteristic crystalline order of silver when unsaturated *cis*-molecules are used. One finds the atomic layer spacing of 0.237, 0.231, 0.226, 0.215, and 0.203 nm, which coincide with the reported values for silver (0.236 and 0.204 nm corresponding to {111} and {200} planes, respectively).[22]

Figures 4, 6, and 8 show the HRTEM and histograms of the particle sizes for eicosenoate, oleate, and palmitoleate, respectively, at a constant $[Ag^+]$/[stabilizer] ratio of 8. They all show rather monodisperse, spherical particles of a rather similar diameter 7.0−7.8 nm (± 1 nm); see Table 3. The monodispersity is manifested also in the 2D hexagonal colloidal assemblies observed in most of the micrographs we scanned. Such ordered arrays were observed in the past for oleate-[13] and thiol-

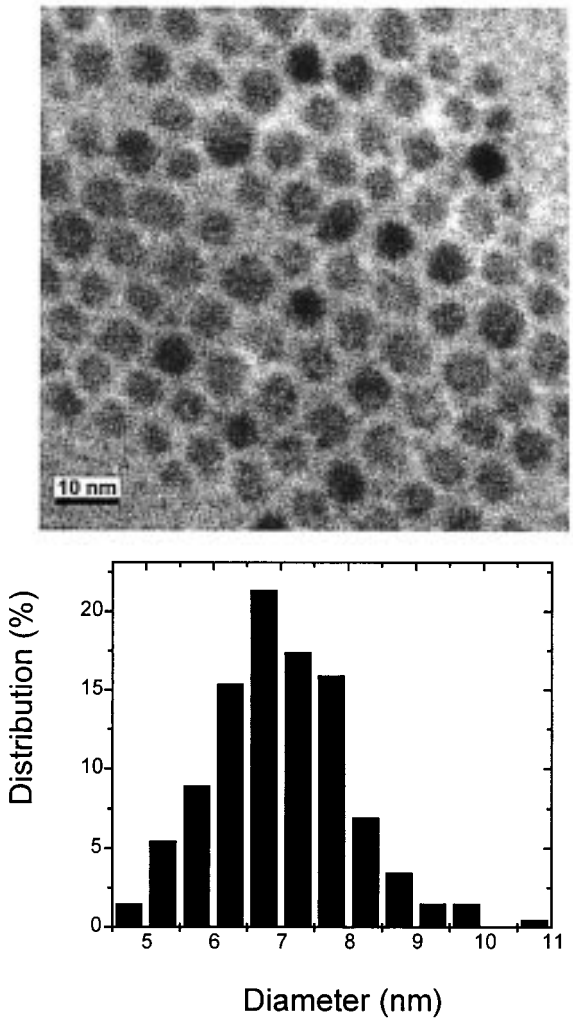

Figure 8. Transmission electron micrograph and histogram of palmitoleate-capped silver particles from a colloidal dispersion in cyclohexane. [Ag]/[stabilizer] = 8.

stabilized[23,24] silver particles, as well as gold[25,26] and semiconductor particles.[27,28]

The concentration of the stabilizer has a significant and systematic effect on the colloidal particle size. The pairs of TEM micrographs, Figures 4 and 5 and Figures 6 and 7, for eicosenoate and oleate, respectively, show that a higher concentration of the stabilizer results in the formation of smaller particles. It is known that additives, such as anisic acid can affect particle nucleation and the subsequent growth.[29] This is also at the basis of some of the modern techniques on colloidal fabrication.[30,31] Our results show this behavior in a straightforward manner for these long-chain (unsaturated) carboxylates. If the presence of the stabilizer does not affect the total amount of the metallic silver, then the radius of the particle should scale with the inverse of the amount of the stabilizer.[29] However, our results show a much smaller dependence, the diameter decreases merely from 7.7 to 5.6−6.1 nm (Table 3) when the $[Ag^+]$/[stabilizer] ratio decreases from 8 to 4. The smaller size ratio (1.3−1.4), compared to the expected 2, might indicate that not all the stabilizer is adsorbed on the silver. Part of it may remain in solution.

We do not find an unambiguous trend in the dependence of the mean particle size on the chain length, for compounds with one double bond. Though the average diameter seems to grow from palmitoleate to eicosenoate (Table 3), the changes are within the experimental uncertainty.

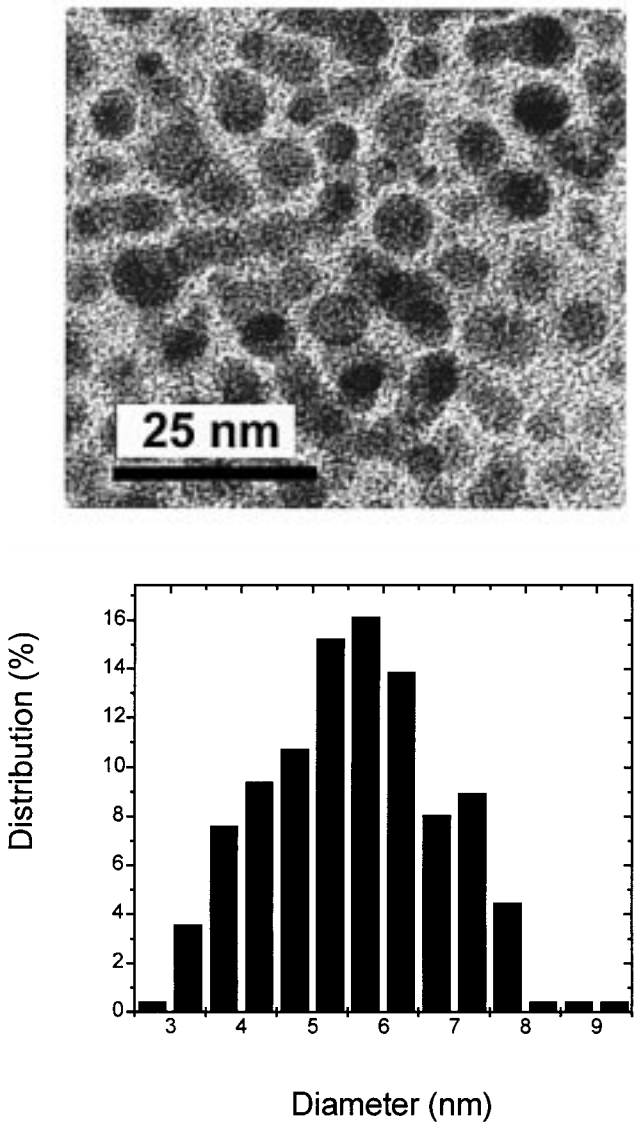

Figure 9. Transmission electron micrograph and histogram of linoleate-capped silver particles from a colloidal dispersion in cyclohexane. [Ag]/[stabilizer] = 8.

In contrast, the presence of additional double bonds in the chain clearly brings about formation of smaller particles (Figures 9 and 10). Two double bonds (linoleate) reduce the particle diameter from ∼7−7.7 nm to ∼5.6 nm, while a third double bond (linolenate) yields particles with a 4.2 nm mean diameter (Table 3). This trend indicates once again that there is a strong interaction between the stabilizers and the silver particles, at all stages of their formation (and stabilization). The larger effect of the two and three double bond molecules over oleate suggests that the polyunsaturated chains lie flat on the surface, taking up more space. This inference is supported by the IR spectra that do not show any residual signal at the positions from ═C−H groups unattached to the surface, but exhibit bands only at higher frequencies.

The shifts registered for the ═C−H stretch of linoleate and linolenate are considerably smaller than those for oleate, eicosenoate, or palmitoleate. This indicates a weaker bonding of the C═C function to the surface, in line with the reduced stability and transfer ratios for these molecules. It appears that the steric and configuration requirements for the simultaneous adsorption of several double bonds strain the double bond/surface binding.

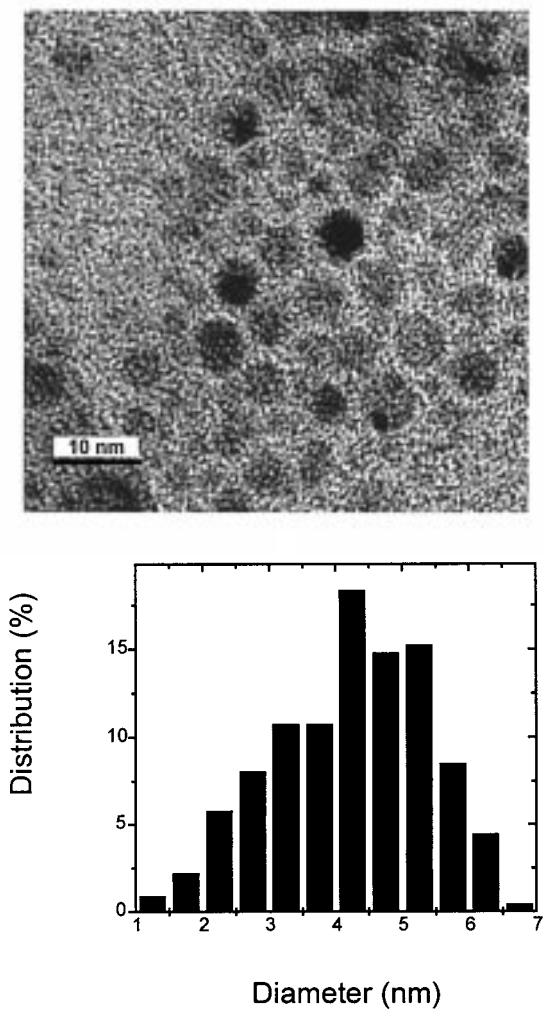

Figure 10. Transmission electron micrograph and histogram of linolenate-capped silver particles from a colloidal dispersion in cyclohexane. [Ag]/[stabilizer] = 8.

TABLE 3: Size Distribution of Silver Particles Dried from Cyclohexane Organosols

stabilizer	[Ag]/[stabilizer] molar ratio	particle size $\langle D\rangle \pm \sigma$, nm	polydispersity $\sigma/\langle D\rangle$
sodium eicosenoate	8:1	7.8 ± 1.6	0.21
	4:1	6.1 ± 0.9	0.15
sodium oleate	8:1	7.7 ± 1.2	0.15
	4:1	5.5 ± 1.2	0.22
sodium palmitoleate	8:1	7.0 ± 1.0	0.15
sodium linoleate	8:1	5.6 ± 1.3	0.23
sodium linolenate	8:1	4.2 ± 1.2	0.27

4. Monolayer and LB Films of the Capped Particles. Silver organosols, such as in chloroform, can spread on the surface of water to form a monoparticulate layer.[32,33] We measure their surface pressure/surface area (π/A) curves. A typical curve is shown in Figure 11. The general shapes of the curves are similar for all the stabilizers we investigate here. The isotherms are quite lacking in structure. The most prominent feature being the collapse. This is similar to previous results.[32,33] The collapse pressures in the π/A isotherms are close to those of the compounds themselves (at pH 5−6). The values of the latter are a little lower than those of the corresponding monoparticulate films (up to 4 mN/m). The particles impart some additional robustness to the film. There is a rough correlation between the collapse pressure of the free stabilizer molecule and that of the capped particle. If this is a real correlation, it may mean that there is indeed a partition of the stabilizer between the

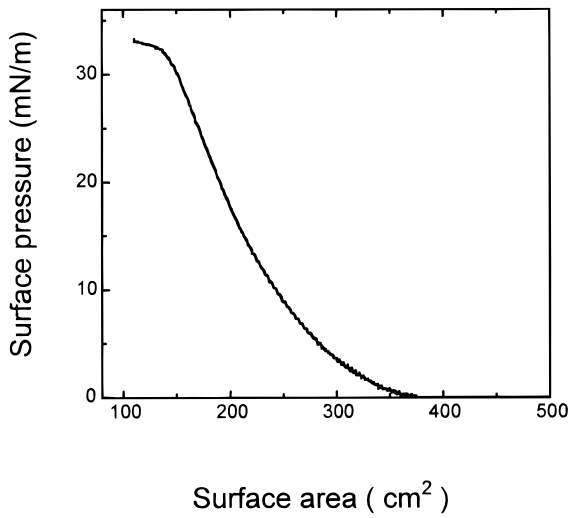

Figure 11. π/A curve for oleate-capped silver colloid spread over water. [Ag] = 1.2×10^{-3} M. 120 μL of a chloroform organosol was spread.

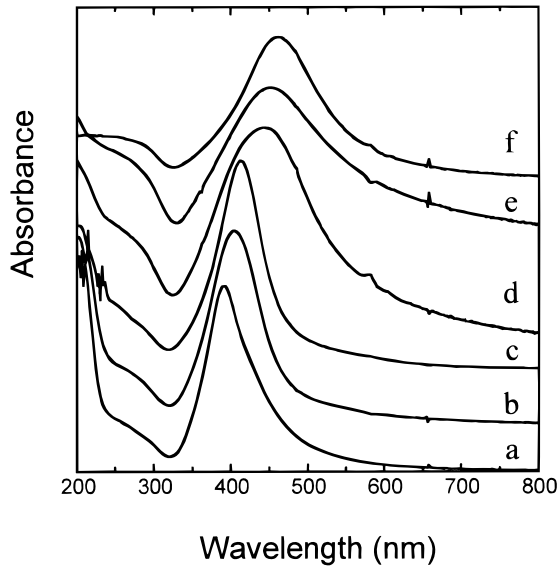

Figure 12. UV−visible spectra of silver nanoparticles: (a) uncapped hydrosol, (b) *cis*-11-eicosenoate-stabilized hydrosol, (c) chloroform organosol from (b), (d) cast film of hydrosol (b), (e) cast film of organosol (c), and (f) LB film from organosol (c).

particle and the liquid surface. Furthermore, the area per particle at collapse is ~1800 nm^2, which is by far much larger than the actual area of a capped particle (~80 nm^2). Thus, the π/A curves are controlled by the free acid stabilizers, filling the large spaces between the particles. This is in agreement with similar findings of Meldrum, Kotov, and Fendler.[33]

Typical UV−visible extinction spectra of the silver particles treated in various ways are compared in Figure 12. The positions of the absorption bands of particulate LB and cast films from hydrosols and organosols are summarized in Table 4. Nearly all the LB films give the same band positioned at 460 ± 2 nm, essentially similar to the cast film of the organosol. The band is broadened and red shifted compared to the bulk colloids, probably due to interparticle interaction in the highly concentrated film. Yet, significant aggregation, which should have been evident in a "tail" extending into the red, is absent. The absorption position does not move as a function of the number of layers, and there is an approximate linear relationship between the number of the LB layers of the oleate-capped particles and the absorption intensity (Figure 13), with a slope approximately

TABLE 4: Extinction Peak Positions in the UV−Visible Spectra of LB and Cast Films of Capped Silver Organosols and Hydrosols

	absorption peak (nm)		
stabilizer	LB film (±2 nm)	organosol cast film (±2 nm)	hydrosol cast film (±10 nm)
sodium eicosenoate	460	462	442
sodium oleate	460	462	432
sodium palmitoleate	460	462	438
sodium linoleate	460	462	444
sodium linolenate	456	448	442
sodium elaidate	460	458	444

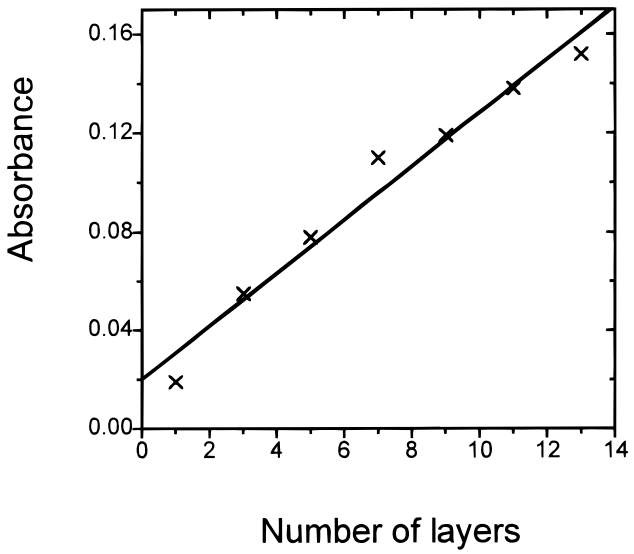

Figure 13. Plasmon absorption intensity as a function of the number of monolayers of oleate-capped silver particles, deposited in a LB film.

1, indicating an efficient transfer of the film from water surface to the solid substrate.

The cast films from silver organosols exhibit absorption maxima near 460 ± 2 nm with few exceptions, and it is almost independent of the concentration of the organosols. The band is shifted to the red compared to the parent suspension, and it is broadened significantly. This behavior seems to be consistent with self-organization in an ordered particle matrix, as has been confirmed by TEM observations (Figures 4−10).

The extinction positions of the hydrosol cast films, however, vary strongly with the type of the surfactant (Table 4) and are sensitive to its concentration. TEM pictures of oleate-capped silver particles have shown that the particles cast from a hydrosol exhibit a smaller degree of self-organization compared to films cast from the organosol.[13]

The deposited LB films or cast films from organosols of all the stabilizers (except stearate, which does not produce an organosol) are quite stable, keeping at room temperature for over 3 months with no change in the absorption spectra. Temperature-dependent absorption spectra of oleate-capped particle LB film do not show any change up to 92 °C. Higher temperature only shifts the absorption maximum to longer wavelength by ∼5 nm, without any noticeable change in the band shape. This means that the particles retain their individual character and are not coagulated, though some changes in the molecular conformation of coating layer seems to occur. A confirmation of the durability of the particles upon heat treatment at 92 °C is the fact that one obtains monodispersed organosols when the treated LB or cast films are washed with the organic solvent. The sharp plasmon peak is regenerated.

Time-dependent π/A curves of an oleate monolayer placed on a hydrosol subphase measured at room temperature are shown in Figure 14. 1×10^{-5} M uncapped silver hydrosol is used as the subphase, and oleic acid is spread over it in chloroform. The apparent area per molecule quickly decreases from ∼0.38 to 0.15 nm^2 in 10 min, and practically to zero in 40 min (Figure 14). Oleate over pure water has a similar behavior; however, the rate of solution is much slower than that over the colloidal subphase (about several hours). This suggests that the colloidal particles collide with the oleate monolayer, coat themselves with an appropriate number of oleate molecules, and "drag" them into the subphase. This process is not controlled by the diffusion of the colloids toward the surface, as we find that the rate depends on the specific stabilizer spread on the subphase.

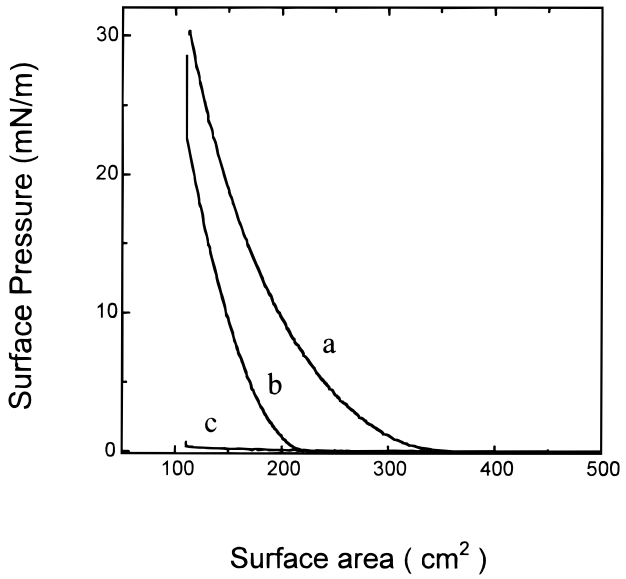

Figure 14. Surface pressure (π)/molecular area (A) curves of an oleic acid monolayer on (a) pure water, (b) 1×10^{-5} M uncapped silver colloidal solution 10 min after spreading, (c) same as (b) but 40 min after spreading. The area per molecule is calculated in terms of the total initial amount of the oleic acid spread on the surface.

As one increases the number of double bonds in the stabilizer chain (from oleate to linolenate), the faster does the dissolution into water and into the colloidal subphase occur. It appears that a single collision of the particle with the monolayer is not sufficient to pull out the maximum amount of molecules. Many collisions are needed or, alternatively, a long residence time of the particle in contact with the film. Another interesting point is that sodium stearate (the saturated molecule) does not dissolve into a silver colloidal subphase. This is further evidence for the importance of bonding of the double bonds of the unsaturated carboxylates to the silver surface in aqueous solution. The C═C double bond plays a crucial role in stabilizing the silver hydrosols and the subsequent induced transfer to organic liquids.

Conclusions

A series of unsaturated carboxylates with different chain length, configuration, and degree of unsaturation are investigated for stabilizing silver nanoparticles. It is found that the size distribution and stability of the Ag particles strongly depend on the type and concentration of the stabilizer. UV−vis and FTIR spectroscopy have confirmed that, though an unsaturated chain is an essential factor for effectively stabilization of the silver particles, the cis configuration is more effective for adsorption of the stabilizer molecule and the transfer of the particles to organic liquids. The cis double bond which is bound

on silver hydrosols can be released after the solvent exchange, while the carboxylate group becomes attached to the surface.

TEM results indicate that smaller particles are obtained with higher stabilizer concentrations and more double bonds in the chain, suggesting a higher coverage by the polyunsaturated chains due to the possible flat packing on the surface.

The important role of cis double bonds on stabilizing the Ag particles is also confirmed by their strong interactions with a colloidal subphase in a Langmuir trough, which is much stronger than for the saturated homologue. These results suggest that cis unsaturated carboxylates are useful stabilizers and phase-transfer switches in Ag nanoparticle preparation.

Acknowledgment. This work was supported by the Israel Science Foundation founded by the Israel Academy of Science and Humanities. X. Chen also acknowledges the financial support from the Chinese Scholarship Council and State Major Basic Research Project of China for his stay in Israel.

References and Notes

(1) (a) Ozin, G. A. *Adv. Mater*. **1992**, *4*, 612. (b) Alivisatos, A. P. *J. Phys. Chem.* **1996**, *100*, 13226. (c) Belloni, J. *Curr. Opin. Colloid Interface Sci.* **1996**, *2*, 184. (d) Brus, L. *Curr. Opin. Colloid Interface Sci.* **1996**, *2*, 197. (e) Fendler, J. H.; Meldrum, F. C. *Adv. Mater.* **1995**, *7*, 607.

(2) (a) Weller, H. *Angew. Chem., Int. Ed. Engl.* **1993**, *32*, 41. (b) Schmidt, G. *Chem. Rev*. **1992**, *92*, 1709. (c) Lewis, L. N. *Chem. Rev*. **1993**, *93*, 2693.

(3) Bahnemann, D. W. *Isr. J. Chem*. **1993**, *33*, 115.

(4) Satoh, N.; Kimura, K. *Bull. Chem. Soc. Jpn*. **1989**, *62*, 1758.

(5) Henglein, A. *J. Phys. Chem*. **1993**, *97*, 5457.

(6) Esumi, K.; Tano, T.; Torigoe, K.; Meguro, K. *Chem. Mater*. **1990**, *2*, 564.

(7) Pileni, M. P.; Lisiecki, I.; Motte, L.; Petit, C.; Cizeron, J.; Moumen, N.; Lixon, P. *Prog. Colloid Polym. Sci*. **1993**, *93*, 1.

(8) Toshima, N.; Yonezawa, T.; Kushihashi, K. *J. Chem. Soc., Faraday Trans*. **1993**, *89*, 2537.

(9) Liz-Marzan, L. M.; Philipse, A. P. *J. Phys. Chem*. **1995**, *99*, 15120.

(10) (a) Sun, T.; Seff, K. *Chem. Rev.* **1994**, *94*, 857. (b) Verykios, X. E.; Stein, F. P.; Coughlin, R. W. *Catal. Rev. Sci. Eng*. **1980**, *22*, 197.

(11) Mostafavi, M.; Marignier, J. L.; Amblard, J.; Belloni, *J. Radiat. Phys. Chem.*. **1989**, *34*, 605.

(12) Matejka, P.; Vlckova, B.; Vohlidal, J.; Pancoska, P.; Baumrunk, V. *J. Phys. Chem*. **1992**, *96*, 1361.

(13) Wang, W.; Efrima, S.; Regev, O. *Langmuir* **1998**, *14*, 602.

(14) Creighton, J. A.; Blatchford, C. G.; Albrecht, M. G. *J. Chem. Soc., Faraday Trans. 2* **1979**, *75*, 790.

(15) Vogel, A. I. *A textbook of Quantitative Inorganic Chemistry*, 3rd ed.; Longamn: London, 1972; pp 79−80.

(16) Creighton, J. A.; Eaton, D. G. *J. Chem. Soc., Faraday Trans.* **1991**, *87*, 3881.

(17) Kawabata, A.; Kubo, R. *J. Phys. Soc. Jpn*. **1966**, *21*, 1675.

(18) Charle, K. P.; Schulze, W. *Ber. Bunsen-Ges. Phys. Chem.* **1984**, *88*, 305.

(19) Kerker, M. *J. Colloid Interface Sci*. **1985**, *105*, 297.

(20) Clothup, N. B.; Daly, L. H.; Wiberley, S. E. *Introduction to Infrared and Raman Spectroscopy*, 2nd Ed.; Academic Press: New York, 1975; Chapters 5, 7, and 9.

(21) Hostetler, M. J.; Stokes, J. J.; Murray, R. W. *Langmuir* **1996**, *12*, 3604.

(22) JCPDS, International Center for Diffraction Data, No. 4-783.

(23) Harfenist, S. A.; Wang, Z. L.; Alvarez, M. M.; Vezmar, I.; Whetten, R. L. *J. Phys. Chem.* **1996**, *100*, 13904.

(24) Taleb, A.; Petit, C.; Pileni, M. P. *Chem. Mater*. **1997**, *9*, 950.

(25) Whetten, R. L.; Khoury, J. T.; Alvarez, M. M.; Murthy, S.; Vezmar, I.; Wang, Z. L.; Cleveland, C. C.; Luedtke, W. D.; Landman, U. *Adv. Mater*. **1996**, *8*, 429.

(26) Brust, M.; Bethell, D.; Schiffrin, D. J.; Kiely, C. J. *Adv. Mater*. **1995**, *7*, 9071.

(27) Murray, C. B.; Kagan, C. R.; Bawendi, M. G. *Science* **1995**, *270*, 1335.

(28) Motte, L.; Billoudet, F.; Lacaze, E.; Douin, J.; Pileni, M. P. *J. Phys. Chem.*. **1997**, *101*, 138.

(29) Burshtain, D.; Zeiri, L.; Efrima, S. *Langmuir*, in press.

(30) Murray, C. B.; Norris, D. J.; Bawendi, M. G.; *J. Am. Chem. Soc*. **1993**, *115*, 8706.

(31) Peng, X.; Wickham, J.; Alivisatos, A. R. *J. Am. Chem. Soc*. **1998**, *120*, 5343.

(32) Efrima, S. *Crit. Rev. Surf. Chem*. **1991**, *1*, 167.

(33) Meldrum, F. C.; Kotov, N. A.; Fendler, J. H. *Mater. Sci. Eng*. **1995**, *C3*, 149.